ELSEVIER

Carbohydrate Research 278 (1995) 11–26

CARBOHYDRATE RESEARCH

The dependence of glucan conformational dynamics on linkage position and stereochemistry

David A. Brant *, Hwa-Song Liu, Zhiqiang S. Zhu

Department of Chemistry, University of California, Irvine, CA 92717-2025, USA

Received 30 November 1994; accepted in revised form 10 June 1995

Abstract

The ^{13}C NMR T_1 relaxation times for the $(1 \rightarrow 4)$-linked maltooligomers (M_i) and the $(1 \rightarrow 6)$-linked isomaltooligomers (IM_i) with $i = 2$, 4, 6, and 8 were measured in aqueous solution at 22 and 65°C at a concentration (3%) low enough to have removed concentration-dependent effects on the measured T_1 values. Separate T_1 values were measured for each carbon in the residue at the reducing end of the oligosaccharide, in the residue at the non-reducing end, and in the interior, i.e., non-terminal, residue(s). Analogous data for the corresponding high polymers show that at 22°C the relaxation times for the carbons of the interior residues of the oligomers have converged to their high chain length asymptotes at about $i = 10$. This observation suggests that at room temperature polymeric motions in the frequency domain effective for ^{13}C NMR relaxation at a magnetic field strength of 11.7 T have a "wavelength" of the order of 10 residues. The relaxation times characterizing the two ends of the chain are different, with longer T_1 values for the carbons of the reducing end than for those of the non-reducing end. Carbons of α-anomeric residues at the reducing end have shorter relaxation times than those of the corresponding β-anomeric reducing sugars. Carbons of the interior residues have T_1 values shorter than the carbons of either type of terminal residue. For oligomers of a given dp there is no T_1 difference between oligomers of the M_i and IM_i series at room temperature. This observation is seemingly at odds with the great differences in the inherent conformational freedom of the $(1 \rightarrow 4)$- and $(1 \rightarrow 6)$-linkages. At elevated temperatures the orientational relaxation behavior of the two series of oligomers measured by ^{13}C T_1 values show interesting differences, and in the case of the M_i series, structure develops in the chain length dependence of the T_1 values.

Keywords: Glucan; Conformational dynamics; Linkage position; Stereochemistry

* Corresponding author.

SSDI 0008-6215(95)00242-1

1. Introduction

Interest in the conformational mobilities of dissolved oligo- and poly-saccharides is currently high [1–21]. In this context it is necessary to distinguish the *extent* of conformational mobility as described, for example, by the equilibrium probability distribution in torsion angle space, from the rate of conformational mobility, which refers in the most elementary sense to the time dependence of transitions among the conformational states represented in this equilibrium distribution. The rates of relaxation to the equilibrium conformational distribution from some non-equilibrium state may also be of interest, for example, in considerations of the viscoelastic properties of polymeric species perturbed by shear from the equilibrium spatial distribution of chain segments.

It is well known that the several types of glycosidic linkage contribute differently to the equilibrium spatial distribution of the oligomer or polymer in which the linkage occurs [22–24]. This effect is evident among homopolysaccharides and the corresponding homooligomers. The vast difference in conformational behavior of α-(1 → 4)-linked amylosic and β-(1 → 4)-linked cellulosic glucans is an often cited case in point [25]. Little is known, however, about possible correlations between linkage type and the rates or dynamics of conformational change [4,9,12,21,26–28]. In this paper we address the latter issue by using ^{13}C NMR relaxation measurements to compare the conformational dynamics of two glucans, amylose and dextran, selected to represent extremes of behavior with respect to the extent of conformational mobility. Representative dimeric segments of amylose and dextran are shown in Fig. 1.

NMR relaxation measurements sample the spectral densities of molecular motions in the laboratory frame at the Larmor frequencies of the subject nuclei or at certain linear combinations of these frequencies [31]. With spectrometers currently in common use this technique then provides a window on modes of molecular motion with Fourier components in the 0.1–1.0 GHz range and characteristic times of the order of 1 ns. For an oligo- or poly-saccharide such modes involve the collective motions of the atoms of one or more sugar residues and clearly include important contributions from significant excursions of the torsion angles about the bonds of the glycosidic linkages [3,32–38]. NMR relaxation is thus an appropriate probe of the dynamics of the changes in molecular conformation, which is most conveniently described in terms of this limited set of internal coordinates [23,25,39].

Here we employ a field strength of 11.7 T for proton-decoupled measurements of ^{13}C NMR longitudinal relaxation times, T_1, which sample the spectral density at $\omega_C = 125$ MHz, $\omega_H - \omega_C = 375$ MHz, and $\omega_H + \omega_C = 625$ MHz, provided relaxation occurs exclusively by dipolar coupling of ^{13}C with the directly bonded hydrogen atom(s) [21,31,40]. Other relaxation parameters provide alternative samplings of the spectral density function [31]. Variations in magnetic field strength allow for sampling the spectral density function at additional frequencies in the 0.1–1 GHz regime [12,21,38], although loss of spectral resolution and sensitivity in the lower reaches of this range limit the usefulness of low frequency NMR for oligo- and poly-saccharides. Other experimental techniques, e.g., infrared [41], fluorescence [42–44], and mechanical [45] spectroscopy, may be used to examine motions in faster and slower time regimes.

Fig. 2 shows a "snapshot" that freezes a segment of a dissolved amylose chain in

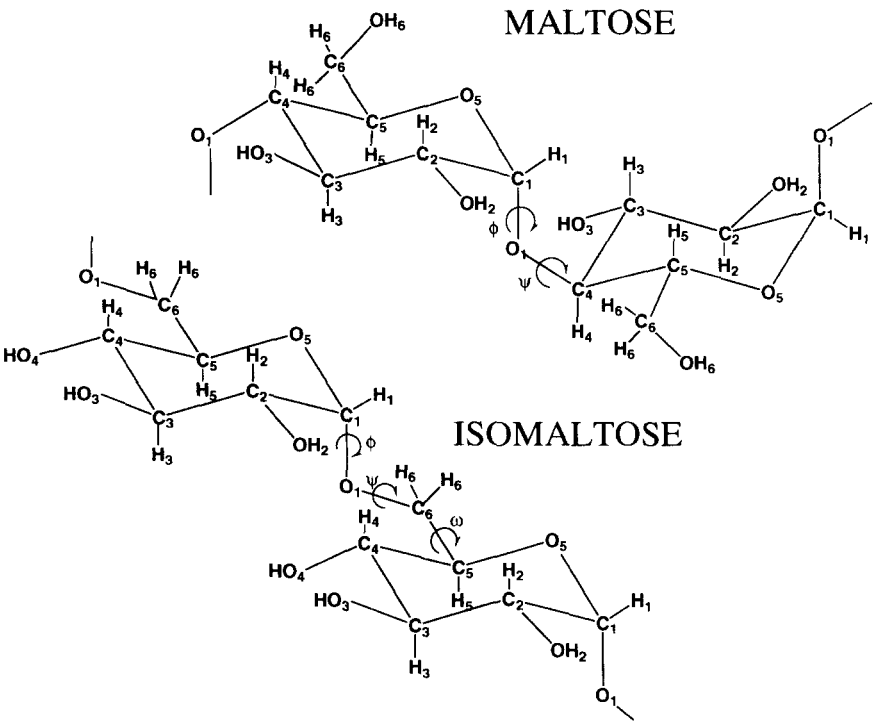

Fig. 1. Characteristic dimeric chain segments, maltose and isomaltose, of the α-(1 → 4)-linked glucan amylose and the α-(1 → 6)-linked glucan dextran, respectively. Torsion angles ϕ, ψ, and ω refer to rotations about bonds of the glycosic linkages as shown; they are defined in detail elsewhere for maltose [29] and isomaltose [30]. Conformations shown are chosen for clarity of illustration and do not necessarily represent low energy forms.

one particular conformation consistent with the equilibrium spatial distribution of the chain. A similar snapshot of a segment of a dextran chain is shown in Fig. 3. These representative chain trajectories were calculated by methods described earlier [24,46] starting from the conformational energy surfaces shown in Figs. 4 and 5. A temperature of 22°C was assumed. Although the helical propensities of the amylosic chain can be clearly contrasted with the absence of helicity in the dextran chain trajectory by comparison of Figs. 2 and 3, inspection of Figs. 4 and 5 provides more compelling evidence for the greater extent of conformational mobility in the α-(1 → 6)-linked dextran chain. Only a small domain in ϕ,ψ space is energetically accessible at ordinary temperatures to maltose, the α-(1 → 4)-linked dimeric segment of amylose (Fig. 4). Much greater conformational freedom is associated with the isomaltose dimer of dextran. Here the linkage region involves three chemical bonds, and, hence, the sugar residues avoid steric conflict over a wide range of ϕ,ψ,ω space. As seen in Fig. 5, there is extensive rotational freedom corresponding to torsion ω about the C5–C6 bond. Moreover, ϕ,ψ cross sections of the three dimensional isomaltose conformational energy surface at any value of ω reveal much more conformational freedom than is

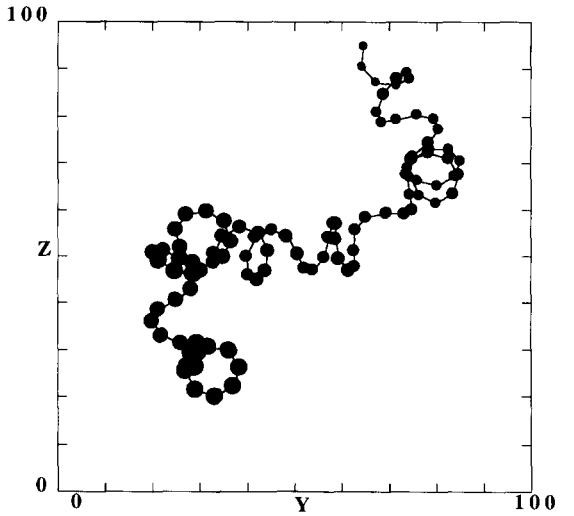

Fig. 2. One conformation of a segment of an α-(1 → 4)-linked glucan chain (amylose) selected from the equilibrium spatial distribution projected into an arbitrary yz plane; the y and z scales are in Å. Circles represent glycosidic oxygens; virtual bonds connecting glycosidic oxygens span the sugar residues, which are not shown. Circle size chosen to simulate x position of oxygens.

found in these same dimensions for maltose.

Conformational features of amylose and dextran can be further differentiated by comparing measures of directional persistence [24,25,49]. Figs. 6 and 7 thus display for amylose and dextran, respectively, the scalar product of virtual bond vector i ($\mathbf{L}_i$) on virtual bond vector $i+j$ ($\mathbf{L}_{i+j}$), normalized by the squared magnitude (L) of the virtual

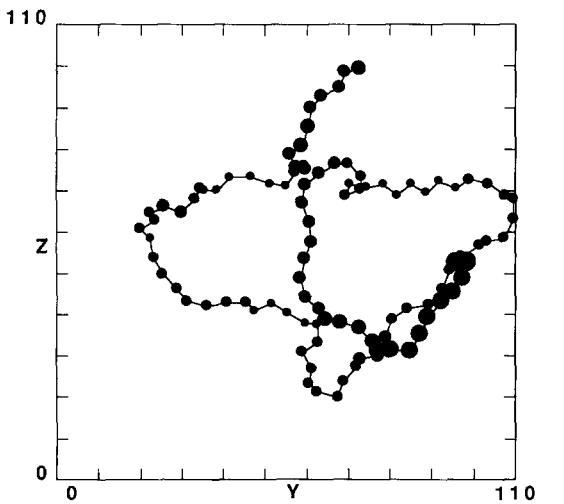

Fig. 3. Same as Fig. 2 but for a segment of an α-(1 → 6)-linked glucan chain (dextran).

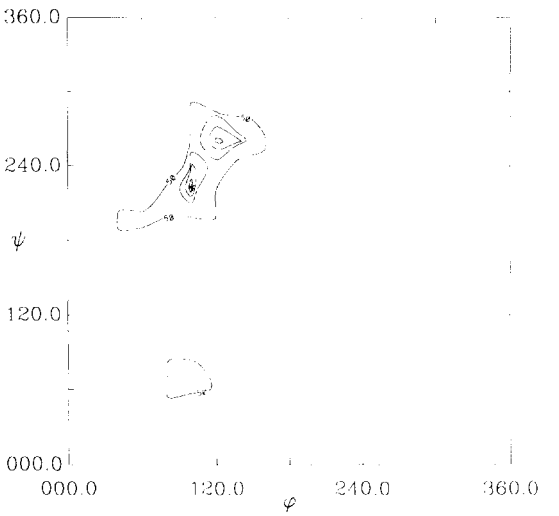

Fig. 4. The conformational energy surface of the α-(1 → 4)-linked glucose disaccharide, maltose. Torsion angles ϕ and ψ are described in Fig. 1. Energy contours plotted 2, 5, 10, and 50 kcal/mol above the global energy minimum were computed for rigid glucose residues at 10° intervals using CHARMm [47] with CHEAT [48] carbohydrate potential functions.

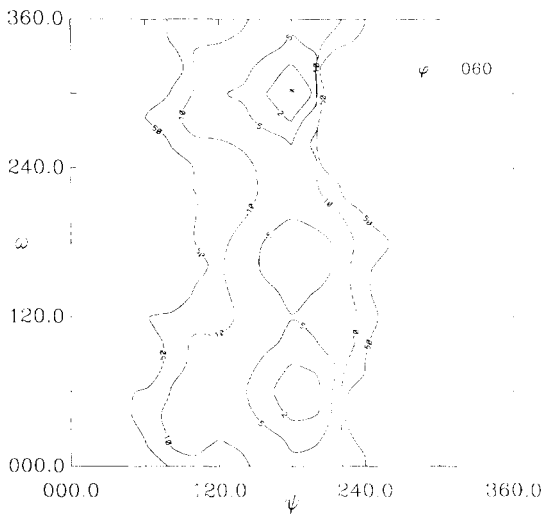

Fig. 5. The conformational energy surface of the α-(1 → 6)-linked glucose disaccharide, isomaltose. Torsion angles ϕ, ψ, and ω are described in Fig. 1. Energy contours plotted 2, 5, 10, and 50 kcal/mol above the global energy minimum were computed for rigid glucose residues at 10° intervals in ψ and ω for $\phi = 60°$ using CHARMm [47] with CHEAT [48] carbohydrate potential functions.

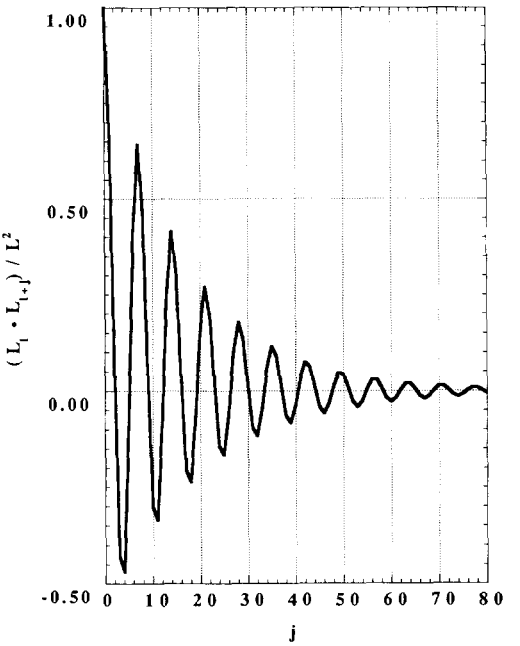

Fig. 6. Directional correlation function of amylose virtual bond vectors i and $i + j$, defined as in the text and plotted against the sequential separation j of the two virtual bonds.

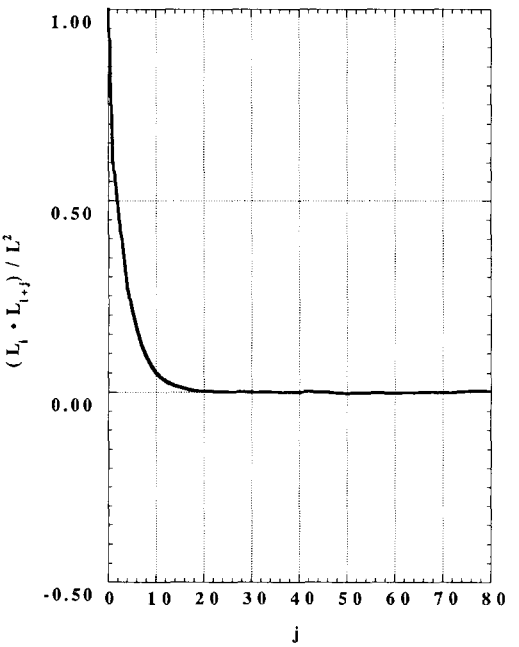

Fig. 7. Same as Fig. 6 for dextran.

bond length and averaged over the ensemble of chain conformations in the equilibrium distribution. This directional correlation function is expected to decline from unity, for the case of perfect correlation $j = 0$, to zero, when j becomes large enough for directional persistence or correlation between bonds i and $i + j$ to have vanished entirely due to the torsional motions of the intervening glycosidic linkages. The oscillatory character of the directional correlation of amylose reflects the ca. six-fold periodicity of its pseudohelical trajectory. Correlation is retained out to beyond $j = 80$ according to the present estimate. For dextran the behavior of each linkage between virtual bonds approaches much closer to that of a universal joint, directional correlation is lost rapidly, and the absence of perceptible periodicity in the correlation function reflects the lack of helical tendency in the chain trajectory.

It must be emphasized that the equilibrium spatial distributions of dissolved amylose and dextran suggested by Figs. 2–7 are based on a model. In particular, the conformational energy surfaces in Figs. 4 and 5 were calculated with CHARMm [47] using the CHEAT potential [48] holding all other internal coordinates fixed as the variables ϕ, ψ, (and ω) were stepped incrementally through the full angular range, and interactions of sugar residues more remote in the chain sequence than first neighbors were ignored [25]. It is not our purpose, nor is it yet possible, to present a complete and quantitatively accurate description of the equilibrium spatial distribution of these chains dissolved in water. We contend, however, that any reasonable model would clearly disclose, and thus help to interpret, the qualitative differences in equilibrium configuration dependent properties of these glucans that are well known from experimental studies [23,24,49–51]. We seek here only to establish clearly the distinction between these two chains in terms of the extent of conformational mobility and the nature of the equilibrium spatial distribution of the chains. In what follows we address the issue of possible differences in the conformational dynamics using ^{13}C NMR relaxation measurements as a probe.

2. Experimental

Procedures.—Maltooligomers (M_i series) were prepared from a commercial sample of enzymatically degraded corn starch (Star-Dri 20, Corn Syrup Solids, A.E. Staley). Isomaltooligomers (IM_i series) were separated from acid-hydrolyzed dextran (T500, Pharmacia). Fractionation of oligomer mixtures was achieved by size exclusion chromatography, and fractions were freeze-dried for storage following procedures already described [1,9]. Experimental attention was restricted here to oligomers with chain length $i = 2$, 4, 6, and 8. The α-cyclodextrin, cyclohexaamylose (cM_6), was purchased from Sigma and used without further purification. Samples for NMR were freeze-dried repeatedly from D_2O solution to exchange hydroxyl protons, dissolved in highly enriched D_2O (99.96%, low paramagnetic contaminants, Aldrich), doped with dioxane as a chemical shift reference, freed of dissolved oxygen by the freeze-thaw technique, and flame-sealed in 5 mm NMR tubes [1]. The oligomer concentration (3 g/dL) was shown previously [9] to be low enough to remove any concentration dependence of the measured T_1 values. All ^{13}C T_1 measurements were made at 11.7 T with a GE GN spectrometer using the standard inversion recovery technique and GE software to extract the relaxation times. Experiments were conducted at 22 ± 1°C and 65 ± 1°C.

Precision and repeatability.—As already reported [9], chemical shift dispersion at 11.7 T was sufficient to distinguish carbons of the ultimate, penultimate, and interior residues of the oligomers. The ^{13}C chemical shifts of all of the carbons of the first five oligomers of the M_i and IM_i series at 22°C, from which the chemical shifts of the terminal, penultimate, and interior residues of the higher oligomers can be deduced, have been reported elsewhere [9]. The chemical shifts are quite insensitive to temperature, and the relative peak positions do not change between 22 and 65°C, so signal assignments at 65°C were straightforward. At 22°C at least ten delay times were used in the inversion recovery procedure, and the recovery kinetics were fit to a three parameter exponential equation [1]. In order to restrict to around 10 h the machine time required for the measurements at 65°C, where T_1 is considerably longer, we used only 6–8 judiciously chosen delay times. The standard deviation in T_1 reported by the GE GN software for fits to a given inversion recovery curve was typically 2–8% of T_1, as we have reported previously [9], and was not perceptibly dependent on the temperature of the experiment. Reproducibility of T_1 values in repeated experiments on the same samples, as measured by the standard deviation of the means of the repeated measurements, was entirely comparable to the standard deviation reported for the exponential fitting of any one inversion recovery experiment. Previously reported T_1 measurements at 22°C [9] were reproduced in the current study within experimental error. We thus take the reproducibility of the present T_1 measurements to be $\pm 5\%$.

Measurements reported.—Given the precision of the present T_1 measurements, it was not possible to distinguish reliably the relaxation times of the several ring carbons of a given ring from one another. Hence, we report here only the mean T_1 for the five endocyclic carbons of a given sugar ring, $\langle T_1 \rangle_{1-5}$. (Inclusion of twice the measured T_1 for C6 had no systematic effect on the average T_1 values, but C6 was nevertheless omitted from the average, because it is part of the main chain backbone in oligomers of the IM_i series but not of the M_i series [1,9].) It was likewise not possible to distinguish the mean relaxation times $\langle T_1 \rangle_{1-5}$ of the endocyclic carbons of the interior sugar rings from those of the penultimate sugar rings. Hence, we report here $\langle T_1 \rangle_{1-5}$ values only for the reducing residues of the oligomers, the non-reducing residues of the oligomers, and the interior residues of the oligomers. The anomeric equilibrium at the reducing ends of the oligomers made it possible to measure $\langle T_1 \rangle_{1-5}$ values for both α- and β-anomeric reducing terminal sugars. Reported uncertainties associated with the $\langle T_1 \rangle_{1-5}$ values, presented as error bars, are the mean values of the standard deviations reported by the fitting algorithm for the five carbons included in the average. We did not measure, and thus do not report, the reproducibilities of all of the measured T_1 values. We estimate, however, that reproducibility error bars would be equal in length to those reported here. Measured values of $\langle T_1 \rangle_{1-5}$ can be read to within the experimental precision from the plots presented, so tabular data are not included.

3. Results and discussion

Chain length and temperature dependence of $\langle T_1 \rangle_{1-5}$.—The measured $\langle T_1 \rangle_{1-5}$ values for the reducing, non-reducing, and interior residues of the M_i and IM_i oligomers

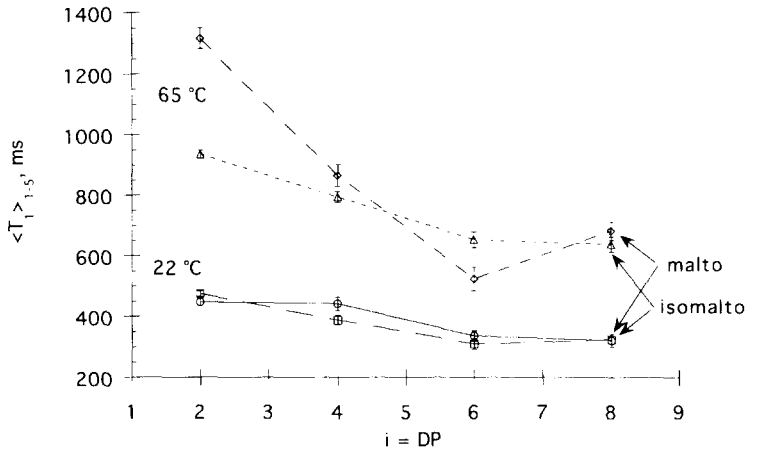

Fig. 8. Plots of $\langle T_1 \rangle_{1-5}$ against chain length i for the reducing residues of the oligomers of the M_i and IM_i series at 22 and 65°C. Data for the α- and β-anomeric forms are averaged together. Error bars have the meaning reported in the "Measurements reported" section of Experimental.

are plotted as functions of oligomer chain length i at 22 and 65°C in Figs. 8–10. Data for the α-cyclodextrin, cM_6, which is the covalently closed cyclic version of M_6, are also shown in Fig. 10 for comparison with the interior residues of the linear maltooligomers. The chain length dependence of all $\langle T_1 \rangle_{1-5}$ values becomes asymptotic at 22°C near $i = 10$. Indeed, we believe the $\langle T_1 \rangle_{1-5}$ values of the interior residues of the oligomers with $i \approx 10$ match those of high polymeric amylose and dextran at room temperature [9]. This observation suggests that the room temperature "wavelength" of the segmental motions of the polymers effective for ^{13}C relaxation at 11.7 T is of the

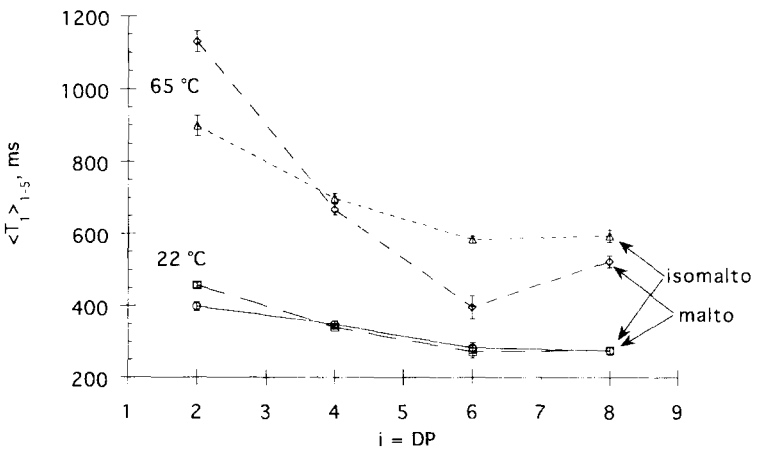

Fig. 9. Plots of $\langle T_1 \rangle_{1-5}$ against chain length i for the non-reducing residues of the oligomers of the M_i and IM_i series at 22 and 65°C. Error bars have the same meaning as in Fig. 8.

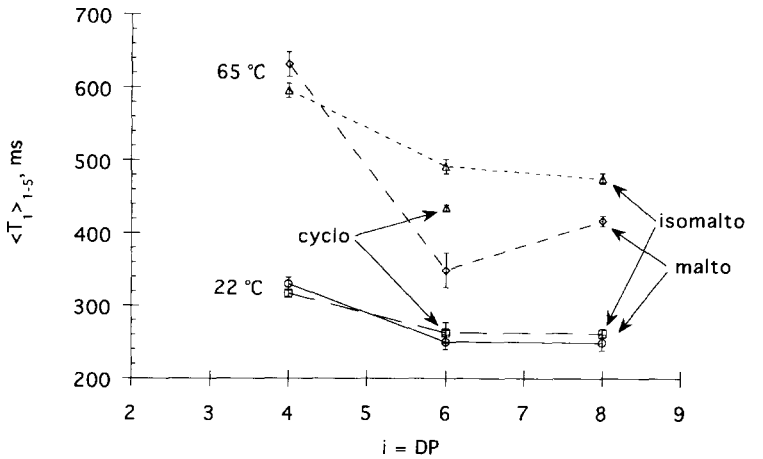

Fig. 10. Plots of $\langle T_1 \rangle_{1-5}$ against chain length i for the interior residues of the oligomers of the M_i and IM_i series at 22 and 65°C; interior residues are not defined for $i < 3$. Data for the α-cyclodextrin cM_6 are also included. Error bars have the same meaning as in Fig. 8.

order of 10 sugars. These segmental motions are those coupled local changes in chain conformation with strong Fourier components at the frequencies ω_C, $\omega_H - \omega_C$, and $\omega_H + \omega_C$ [3,32–38]. At 65°C the data for the IM_i oligomers also suggest an asymptotic approach to high polymer behavior near $i = 10$, but in this case we have no data corresponding to $i > 10$, so asymptotic behavior cannot be concluded with similar confidence. Indeed, the minimum at $i = 6$ in the chain length dependence of all three $\langle T_1 \rangle_{1-5}$ values for the M_i series at 65°C encourages caution with respect to any conclusion regarding the wavelength of segmental motions at the higher temperature.

At room temperature there is no difference in the ^{13}C $\langle T_1 \rangle_{1-5}$ values for the oligomers with corresponding chain length in the M_i and IM_i series, a conclusion reported earlier on the basis of less extensive evidence [9]. Likewise, $\langle T_1 \rangle_{1-5}$ for cM_6 is identical with that for the two linear hexamers at 22°C. These findings are interesting, indeed surprising, in view of the evident differences in extent of conformational mobility and equilibrium spatial distribution of the malto- and isomalto-oligomers described above. The $\langle T_1 \rangle_{1-5}$ values of terminal residues are consistently larger than those of interior residues. Except for the M_i series at 65°C, all $\langle T_1 \rangle_{1-5}$ values decrease with increasing chain length of the oligomer. These observations suggest that, in the dynamics regime governing ^{13}C T_1 values at 11.7 T, faster and/or more extensive molecular motions lead to longer $\langle T_1 \rangle_{1-5}$ values. This conclusion is consistent with the observation (Figs. 8–10) that all $\langle T_1 \rangle_{1-5}$ values increase with increasing temperature. Taken together, these observations imply that the pertinent molecular motions approach the "extreme narrowing" regime and that the oligomers do not behave dynamically as rigid bodies [32,34].

Comparison of reducing and non-reducing chain ends.—Reducing terminal $\langle T_1 \rangle_{1-5}$ values are consistently longer than those of the corresponding non-reducing sugars, as shown in Fig. 11 for both series of oligomers and at both temperatures. Longer $\langle T_1 \rangle_{1-5}$

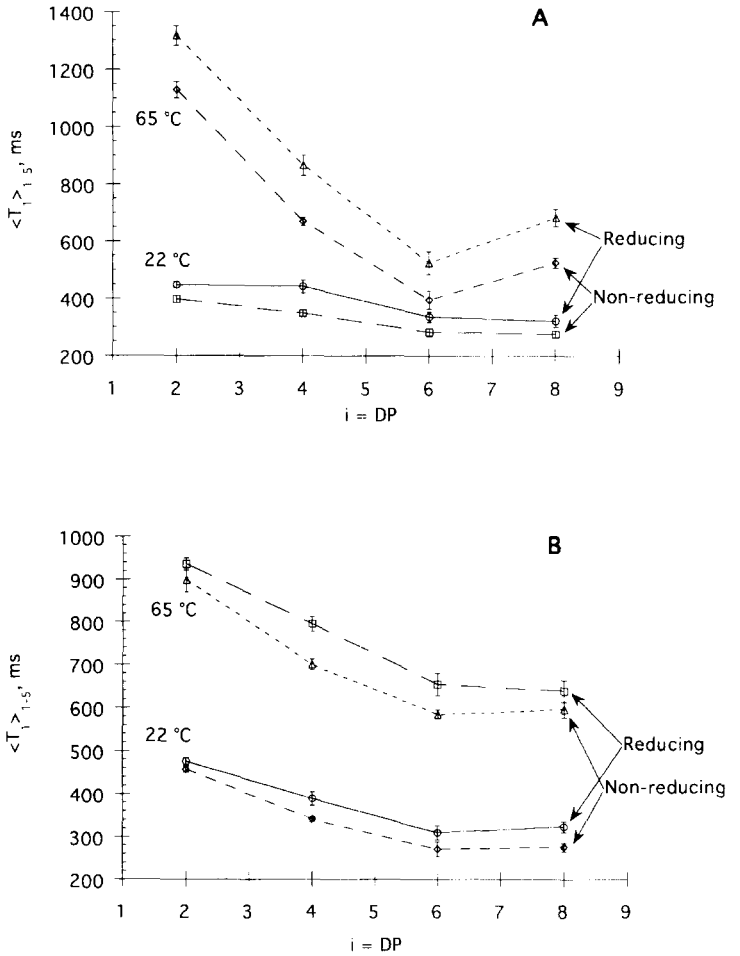

Fig. 11. Plots of $\langle T_1 \rangle_{1-5}$ against chain length i for the reducing and non-reducing terminal residues of the oligomers of the M_i (A) and IM_i (B) series at 22 and 65°C. Error bars have the same meaning as in Fig. 8.

values have also been observed for the reducing sugars of oligomers derived from the copolymeric glucan, pullulan, which contains both α-(1 → 4)- and α-(1 → 6)-linkages [1]. This is a general characteristic of all of the carbons of the reducing residues of these three series of glucan oligomers, and is not simply the result of an especially strong influence on $\langle T_1 \rangle_{1-5}$ from the anomeric carbon. We have speculated that this effect may be related to the existence of the anomeric equilibrium at the reducing end [1,9], but detailed dynamic modeling would probably be required, perhaps including the possibility for opening and closing of the reducing terminal sugar ring, to provide a molecular interpretation of this observation. A longer $\langle T_1 \rangle_{1-5}$ has also been observed for the reducing residue of the 1-*O*-methylated heparin pentasaccharide than for the non-reducing terminal sugar [21]. In this case, where the anomeric equilibrium is not an issue, the

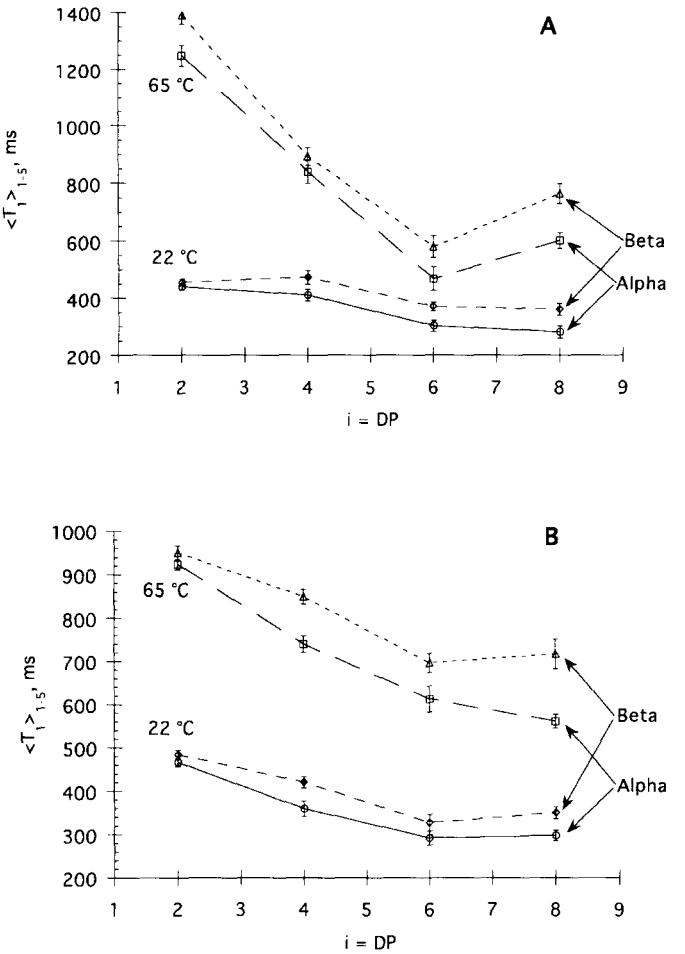

Fig. 12. Plots of $\langle T_1 \rangle_{1-5}$ against chain length i for the α- and β-anomeric forms of the reducing residues of the oligomers of the M_i (A) and IM_i (B) series at 22 and 65°C. Error bars have the same meaning as in Fig. 8.

apparent "extra mobility" associated with the reducing terminus might well be a consequence of the occurrence of the flexible iduronic acid residue adjacent to the reducing terminus. In contrast to these observations, the fully acetylated oligomers derived from cellulose display longer $\langle T_1 \rangle_{1-5}$ values for the non-reducing termini [5].

Comparison of α- and β-anomeric reducing residues.—Fig. 12 shows that the β-anomeric reducing residues have $\langle T_1 \rangle_{1-5}$ values consistently longer than those of the corresponding α-anomeric reducing residues for both series of oligomers and at both temperatures. Again, this is a property of all of the carbons of the residue and not a special feature of the anomeric carbon. We have earlier observed longer $\langle T_1 \rangle_{1-5}$ values for the β-terminal residue than for the α-anomer for these two series of oligomers in measurements at higher concentration [9]. We did not observe this in the relaxation

Table 1
Root-mean-square unperturbed end-to-end distance $\langle r^2 \rangle_0^{1/2}$ of oligomers M_i and IM_i at 22 and 65°C estimated from energy surfaces in Figs. 4 and 5 [a]

i	22°C		65°C	
	M_i	IM_i	M_i	IM_i
2	8.16	8.63	8.15	8.57
4	12.23	15.47	12.15	15.32
6	13.28	21.38	12.82	21.11
8	16.06	26.55	15.07	26.18

[a] Distances in Å.

times associated with the α- and β-anomeric terminal residues in measurements of the oligomers of pullulan at lower magnetic field strengths [1].

4. Conclusions

The greater inherent conformational freedom of the α-(1 → 6) linkage of the IM_i series relative to that of the α-(1 → 4)-linkage of the M_i series is evident from Figs. 2–7. This inherent flexibility difference is not detectable in the $\langle T_1 \rangle_{1-5}$ values measured at 11.7 T at room temperature. Although T_1 measurements at a single field strength do not sample the power spectrum of molecular motions very thoroughly, it seems safe to conclude that large differences in internal motions on the pertinent ns timescale that might arise from structural differences in the two classes of oligomers are suppressed in aqueous solution at room temperature. Viscous effects on the rates of motion, which are common to the two sets of oligomers, may dominate structural effects in this medium.

The root-mean-square unperturbed end-to-end distances $\langle r^2 \rangle_0^{1/2}$ of the several oligomers have been estimated from the energy surfaces in Figs. 4 and 5 by averaging over appropriate Monte Carlo samples [46]. These are presented in Table 1, where it is seen that the mean overall dimensions of the M_i and IM_i oligomers of a given chain length differ significantly for $i > 2$ at 22 and 65°C, consistent with the rather different character of the equilibrium spatial distribution of chain segments. The small incremental change in $\langle r^2 \rangle_0^{1/2}$ for the M_i series in passing from $i = 4$ to $i = 6$ reflects the six-fold pseudohelical chain trajectory of the α-(1 → 4)-linked chain that is imposed by the highly constrained energy surface in Fig. 4. This effect is not so dramatic, if an energy surface relaxed with respect to all internal coordinates except ϕ and ψ is used to compute $\langle r^2 \rangle_0^{1/2}$.

It is evident that one cannot explain the similarities in T_1 for the corresponding members of M_i and IM_i at room temperature by postulating that any two corresponding oligomers have effectively the same overall dimensions and execute essentially rigid body rotations with very similar rotational correlation times. Instead, it appears that the more extended IM_i oligomers, for which the overall rotational diffusion must be slower than for the corresponding member of the M_i series, may gain some compensating higher frequency contributions to the power spectrum from motions along the internal

degrees of freedom. It would not be correct to conclude, however, that the M_i oligomers behave as rigid bodies under these conditions. The readily detectable dynamic distinction between terminal and interior residues and, especially, the approach of $\langle T_1 \rangle_{1-5}$ to an asymptote near $i = 10$ indicate that internal motions play a role in determining the relaxation behavior of both series of oligomers.

At temperatures sufficiently greater than 22°C one might expect that reduction in the solvent viscosity and the opportunity provided at the larger thermal energies for the molecules to explore a wider domain in the torsional configuration space would permit differences in the inherent conformational freedom of the glycosidic linkages to be revealed in the relative values of $\langle T_1 \rangle_{1-5}$ for the two series. In particular, it might be anticipated that the $\langle T_1 \rangle_{1-5}$ values for members of the IM_i series would begin to exceed those for the corresponding members of the M_i series, owing to the structural differences evident in Figs. 2–7.

These expectations are only partially realized in the data at 65°C. Of the eleven direct comparisons that can be made from Figs. 8–10, $\langle T_1 \rangle_{1-5}$ for a member of the IM_i series exceeds that for the corresponding M_i oligomer in just five cases, if we take the $\pm 5\%$ reproducibility of the measurements into account. The "rule" is violated already for $i = 2$, where $\langle T_1 \rangle_{1-5}$ for M_2 substantially exceeds that for IM_2 at 65°C for both the reducing and non-reducing residues. This observation might be rationalized on grounds that the α-(1 → 4)-linked M_2 is more compact than IM_2 (Table 1), but the calculated difference in $\langle r^2 \rangle_0^{1/2}$ for M_2 and IM_2 scarcely seems large enough to explain the relatively large difference observed in T_1 for this pair at 65°C. All of the plots of $\langle T_1 \rangle_{1-5}$ vs i in Figs. 8–10 show a crossover at $i = 4$ to bring the data into general conformity with the rule at $i = 6$, but there are strong hints that the rule is, in fact, the exception in the evidence that the curves may cross again at $i = 8$.

The minima in these plots at $i = 6$ for the M_i oligomers may be related to the approximately six-fold periodicity of the amylose pseudohelical chain trajectory. If this were the case, however, one might have expected a rather longer T_1 for the roughly circular, and quite compact, M_6 species. Indeed, a maximum in $\langle T_1 \rangle_{1-5}$ at $i = 6$ for the M_i series might have been expected instead of a minimum. The relative magnitudes of $\langle T_1 \rangle_{1-5}$ for M_6 and cM_6 are also interesting. On the one hand it might be argued that because cM_6 is probably more compact and, thus, has a shorter rotational correlation time than M_6, its longer $\langle T_1 \rangle_{1-5}$ is expected. On the other hand the additional internal flexibility available to M_6 might have been expected to lead to longer $\langle T_1 \rangle_{1-5}$ values for M_6 than for cM_6. It is evident that the results embodied in Figs. 8–10 will require consideration of detailed models to achieve a satisfying molecular interpretation. It is our impression that conventional models that treat the oligomers as rigid bodies [52,53], or as rigid bodies with faster moving flexible constituents [3,54,55], will not suffice to explain the current observations.

Acknowledgements

We acknowledge with thanks the guidance and technical assistance provided by Drs Mehran Kadkhodaei and Jiejun Wu. This work has been supported by NIH Research Grant GM33062.

References

[1] A.J. Benesi and D.A. Brant, *Macromolecules*, 18 (1985) 1109–1116.
[2] D.C. McCain and J.L. Markley, *J. Am. Chem. Soc.*, 108 (1986) 4259–4264.
[3] P. Dais, *Carbohydr. Res.*, 160 (1987) 73–93.
[4] D.A. Cumming and J.P. Carver, *Biochemistry*, 26 (1987) 6676–6683.
[5] C.M. Buchanan, J.A. Hyatt, S.S. Kelley, and J.L. Little, *Macromolecules*, 23 (1990) 3747–3755.
[6] Z.Y. Yan and C.A. Bush, *Biopolymers*, 29 (1990) 799–811.
[7] S. Homans, *Biochemistry*, 29 (1990) 9110–9118.
[8] C.J. Edge, V.C. Singh, R. Bazzo, G.L. Taylor, R.A. Dwek, and T.W. Rademacher, *Biochemistry*, 29 (1990) 1971–1974.
[9] M. Kadkhodaei, H. Wu, and D.A. Brant, *Biopolymers*, 31 (1991) 1581–1592.
[10] G. Widmalm, R.A. Byrd, and W. Egan, *Carbohydr. Res.*, 229 (1992) 195–211.
[11] L. Poppe and H. van Halbeek, *J. Am. Chem. Soc.*, 114 (1992) 1092–1094.
[12] M. Hricovini, R.N. Shah, and J.P. Carver, *Biochemistry*, 31 (1992) 10018–10023.
[13] J.W. Brady and R.K. Schmidt, *J. Phys. Chem.*, 97 (1993) 958–966.
[14] L.M.J. Kroon-Batenburg, J. Kroon, B.R. Leeflang, and J.F.G. Vliegenthart, *Carbohydr. Res.*, 245 (1993) 21–42.
[15] P.J. Hajduk, D.A. Horita, and L.E. Lerner, *J. Am. Chem. Soc.*, 115 (1993) 9196–9201.
[16] B.J. Hardy and A. Sarko, *J. Comput. Chem.*, 14 (1993) 848–857.
[17] C.A. Bush, *Biophys. J.*, 66 (1994) 1267–1268.
[18] L. Poppe, H. van Halbeek, D. Acquotti, and S. Sonnino, *Biophys. J.*, 66 (1994) 1642–1652.
[19] H. Desvaux and M. Goldman, *Mol. Phys.*, 81 (1994) 955–974.
[20] C. Mukhopadhyay, K.E. Miller, and C.A. Bush, *Biopolymers*, 34 (1994) 21–29.
[21] M. Hricovini and G. Torri, *Carbohydr. Res.*, 268 (1995) 159–175.
[22] D.A. Rees, *Polysaccharide Shapes*, Chapman and Hall, London, 1977.
[23] D.A. Brant, in J. Preiss (Ed.), *The Biochemistry of Plants*, Academic Press, New York, 1980, Vol. 3, pp 425–472.
[24] B.A. Burton and D.A. Brant, *Biopolymers*, 22 (1983) 1769–1792.
[25] D.A. Brant and M.D. Christ, in A.D. French and J.W. Brady (Ed.), *Computer Modeling of Carbohydrate Molecules*, American Chemical Society, Washington, DC, 1990, Vol. 430, pp 42–68.
[26] K. Matsuo, *Macromolecules*, 17 (1984) 449–452.
[27] D. Gagnaire, S. Perez, and V. Tran, *Makromol. Chem.*, 185 (1984) 829–837.
[28] D.A. Cumming and J.P. Carver, *Biochemistry*, 26 (1987) 6664–6676.
[29] S.N. Ha, L.J. Madsen, and J.W. Brady, *Biopolymers*, 27 (1988) 1927–1952.
[30] I. Tvaroska, A. Imberty, and S. Perez, *Biopolymers*, 30 (1990) 369–379.
[31] J.W. Peng and G. Wagner, *J. Magn. Reson.*, 98 (1992) 308–332.
[32] F. Heatley, *Prog. Nucl. Magn. Res. Spectrosc.*, 13 (1979) 47–85.
[33] G.T. Evans, in J.M. Haile and G.A. Mansoori (Ed.), *Molecular-Based Study of Fluids*, American Chemical Society, Washington, DC, 1983, Vol. 204, pp 423–444.
[34] F.A. Bovey and L.W. Jelinski, *J. Phys. Chem.*, 89 (1985) 571–583.
[35] A. Perico, *Acc. Chem. Res.*, 22 (1989) 336–342.
[36] A. Perico, *Biopolymers*, 28 (1989) 1527–1540.
[37] M.M. Fuson, D.J. Anderson, F. Liu, and D.M. Grant, *Macromolecules*, 24 (1991) 2594–2597.
[38] D.J. Gisser, S. Glowinkowski, and M.D. Ediger, *Macromolecules*, 24 (1991) 4270–4277.
[39] D.A. Brant, *Q. Rev. Biophys.*, 9 (1976) 527–596.
[40] R.M. Levy, M. Karplus, and P.G. Wolynes, *J. Am. Chem. Soc.*, 103 (1981) 5998–6011.
[41] T.J. Johnson, A. Simon, J.M. Weil, and G.W. Harris, *Appl. Spectrosc.*, 47 (1993) 1376–1381.
[42] S. Kitamura and T. Kuge, *Food Hydrocolloids*, 3 (1989) 313–326.
[43] Y. Hu, G.R. Fleming, K.F. Freed, and A. Perico, *Chem. Phys.*, 158 (1991) 395–408.
[44] K.G. Rice, P. Wu, L. Brand, and Y.C. Lee, *Curr. Opin. Struct. Biol.*, 3 (1993) 669–674.
[45] C.J. Carriere, E.J. Amis, J.L. Schrag, and J.D. Ferry, *J. Rheol.*, 37 (1993) 467–478.
[46] R.C. Jordan, D.A. Brant, and A. Cesáro, *Biopolymers*, 17 (1978) 2617–2632.

[47] B.R. Brooks, R.E. Bruccoleri, B.D. Olafson, D.J. States, S. Swaminathan, and M. Karplus, *J. Comput. Chem.*, 4 (1983) 187–217.
[48] P.D.J. Grootenhuis and C.A.G. Haasnoot, *Mol. Simul.*, 10 (1993) 75–95.
[49] G.S. Buliga and D.A. Brant, *Int. J. Biol. Macromol.*, 9 (1987) 77–86.
[50] D.A. Brant (Ed.), *Solution Properties of Polysaccharides*, American Chemical Society, Washington, DC, 1981, Vol. 150.
[51] G.S. Buliga and D.A. Brant, *Int. J. Biol. Macromol.*, 9 (1987) 71–76.
[52] J. Lyerla J.R. and G.C. Levy, in G.C. Levy (Ed.), *Topics in Carbon-13 NMR Spectroscopy*, Wiley, New York, 1974, Vol. 1, pp 79–148.
[53] M. Goldman, *Quantum Description of High-Resolution NMR in Liquids*, Clarendon, Oxford, 1988.
[54] D.E. Woessner, *J. Chem. Phys.*, 36 (1962) 1–4.
[55] G. Lipari and A. Szabo, *J. Am. Chem. Soc.*, 104 (1982) 4546–4559.